Disorder and Impurities in Hubbard-Antiferromagnets

M. Ulmke[1], P.J.H. Denteneer[2], V. Janiš[3], R.T. Scalettar[4], A. Singh[1,*], D. Vollhardt[1], and G.T. Zimanyi[4]

[1] Theoretische Physik III, Elektronische Korrelationen und Magnetismus, Institut für Physik, Universität Augsburg, 86135 Augsburg, Germany
[2] Lorentz Institute for Theoretical Physics, University of Leiden, P.O. Box 9506, 2300 RA Leiden, The Netherlands
[3] Institute of Physics, Academy of Sciences of the Czech Republik, CZ 18040 Praha 8, Czech Republik
[4] Department of Physics, University of California, Davis, CA 95616, USA
* On leave from Department of Physics, Indian Institute of Technology, Kanpur 208016.

Abstract: We study the influence of disorder and randomly distributed impurities on the properties of correlated antiferromagnets. To this end the Hubbard model with (i) random potentials, (ii) random hopping elements, and (iii) randomly distributed values of interaction is treated using quantum Monte Carlo and dynamical mean-field theory. In cases (i) and (iii) weak disorder can lead to an enhancement of antiferromagnetic (AF) order: in case (i) by a disorder-induced delocalization, in case (iii) by binding of free carriers at the impurities. For strong disorder or large impurity concentration antiferromagnetism is eventually destroyed. Random hopping leaves the local moment stable but AF order is suppressed by local singlet formation. Random potentials induce impurity states within the charge gap until it eventually closes. Impurities with weak interaction values shift the Hubbard gap to a density off half-filling. In both cases an antiferromagnetic phase without charge gap is observed.

1 Introduction

Antiferromagnetic spin correlations are present in many strongly correlated electron systems, notably the prototype Mott insulators NiO and V_2O_3, the parent compounds of HTSC cuprates, and heavy fermion systems such as YbP, U_2Zn_{17}, and many others. Many of those systems are intrinsically disordered, in particular upon additional homo- or heterovalent doping. The influence of impurity doping on antiferromagnetic (AF) order and electronic properties has recently been studied in a variety of systems. Doping with static scatterers like nonmagnetic impurities usually weakens antiferromagnetic order, a prominent example being Zn doping in $YBa_2Cu_3O_6$ [1]. In spin chains ($CuGeO_3$) [2] and ladder compounds ($SrCu_2O_3$) [3] doping with magnetic and nonmagnetic impurities can *induce* AF order while the pure systems show spin gap behavior. Very effective in destroying AF order are mobile carriers, e.g. hole doping in $La_{1-x}Sr_xCuO_4$ [4]. The stability of AF order strongly depends on the positions of the dopant level. While in the nickel oxides $La_{1-x}Sr_xNiO_4$ [5] and $Ni_{1-x}Li_xO$ [6] holes are supposed to be localized, in the cuprate

$La_{1-x}Sr_xCuO_4$ the hole level lies in the valence band leading to mobile scatterers. As a result, AF order is stable in $La_{1-x}Sr_xNiO_4$ up to $x = 0.5$, but is destroyed in the cuprate already at approx. 5% Sr doping.

In the present paper, we will study the influence of disorder on AF order and the Mott band gap in correlated antiferromagnets. We employ the Hubbard model in the presence of different types of disorder. While the (disordered) Hubbard model is certainly far too simple to describe real materials it already contains very rich physics including local moment formation, magnetic ordering, Mott-Hubbard transition, and Anderson localization. On the other hand, the interplay of disorder and interactions in electronic systems belongs to the most difficult problems in physics, and reliable results within simple models are still very desirable. The problem has been investigated in the past by a variety of methods, including field theoretical approaches [7], renormalization group treatments [8,9], unrestricted Hartree-Fock [10,11], dynamical mean-field theory (DMFT) [12–14], quantum Monte Carlo (QMC) [15–17], and several more (see [18] for a review). Here, we give an overview of results obtained by QMC and DMFT concentrating on the AF phase diagram and the Mott gap.

We consider the following Hubbard Hamiltonian

$$\hat{H} = \sum_{i\sigma}(\varepsilon_i - \mu)\hat{n}_{i\sigma} + \sum_{\langle ij\rangle\sigma} t_{ij}(\hat{c}^{\dagger}_{i\sigma}\hat{c}_{j\sigma} + \text{h.c.}) + \sum_i U_i(\hat{n}_{i\uparrow} - \frac{1}{2})(\hat{n}_{i\downarrow} - \frac{1}{2}). \tag{1.1}$$

In principle all parameters $\varepsilon_i, t_{ij}, U_i$ can be randomly distributed. The precise definition of the different disorder types studied in this paper will be given in the following sections. The average $t \equiv \langle t_{ij}\rangle$ sets our energy scale. We will restrict the hopping t_{ij} to nearest-neighbors hence not allowing for frustration. Longer range, random hopping amplitudes will be important in the modeling of amorphous materials such as doped semiconductors [18,19] and are not considered in the present work.

2 Methods

2.1 Determinant Quantum Monte Carlo (*d*=2)

We use a finite temperature determinant quantum Monte Carlo method [20] to obtain approximation-free results for finite lattices. The algorithm is based on a mapping of the interacting electron problem onto a $d+1$ dimensional quasi-classical problem using auxiliary Ising-type spins. It provides for calculating thermal averages of observables, $\hat{A}$, at a temperature $T = 1/\beta$,

$$\langle\hat{A}\rangle = \frac{\mathrm{Tr}\hat{A}e^{-\beta\hat{H}}}{\mathrm{Tr}e^{-\beta\hat{H}}}. \tag{2.2}$$

The phase space sampling over the auxiliary field configurations is performed using Monte Carlo techniques. The weight of a configuration is proportional to a product of two determinants, one for each electron spin species. In the case of half-filling without random potentials, i.e. $\varepsilon_i - \mu \equiv 0$, on a bipartite lattice the determinants always have the same sign, hence their product is always positive semi-definite, which can be shown by particle-hole transformation of one spin species $[c_{\vec{i}\downarrow} \to (-1)^{\vec{i}} c^{\dagger}_{\vec{i}\downarrow}]$. In the general situation that the product can become negative the algorithm can still be employed in principle. However, the signal to noise ratio decreases exponentially with systems size, inverse temperature, and interaction, putting severe restrictions to the applicability of the method. This so-called "minus-sign problem" is a general obstacle for all exact fermionic Monte Carlo methods as well as for spin-systems in the presence of frustration. Even without the minus-sign problem the computational effort is large because the computer time grows cubically with system size N, restricting N to the order of 100 on present supercomputers.

In the case of disorder all observables have to be averaged over the (frozen) disorder configurations. Because of the computational effort we restrict ourselves to two dimensional lattices with linear size up to $L_x = 10$ which often allows a reliable finite size scaling. Since we are interested in AF ordering we calculate the magnetic correlation functions $C(\vec{l})$ and their Fourier transforms, the magnetic structure factors $S(\vec{q})$,

$$C(\vec{l}) = \frac{1}{N}\sum_{\vec{j}} \langle m_{\vec{j}} m_{\vec{j}+\vec{l}} \rangle, \quad S(\vec{q}) = \sum_{l} C(\vec{l}) e^{i\vec{q}\vec{l}}. \tag{2.3}$$

In particular the AF structure factor $S(\pi,\pi)$ is used to obtain the ground state sublattice magnetization M by a finite size scaling Ansatz according to spinwave theory [21]:

$$\frac{S(\pi,\pi)}{N} = \frac{M^2}{3} + O(\frac{1}{L_x}). \tag{2.4}$$

2.2 Dynamical Mean-Field Theory (Limit of Infinite Dimensions)

The dynamical mean-field theory [22,23] is a local approximation in which the self energy becomes site diagonal, or momentum independent:

$$\Sigma_{ij}(\omega) = \delta_{ij}\Sigma(\omega), \qquad \tilde{\Sigma}(\vec{k},\omega) = \tilde{\Sigma}(\omega). \tag{2.5}$$

The one-particle Green function $G(\vec{k},\omega)$ can hence be obtained from the non-interaction Green function $G^0(\vec{k},\omega)$ by $G(\vec{k},\omega) = G^0(\vec{k},\omega - \tilde{\Sigma}(\omega))$, and the local Green function is given by $G_{ii}(\omega) = 1/N\sum_{\vec{k}} G(\vec{k},\omega)$ This does not imply a simple shift of energies, like in traditional mean-field theories (e.g. Hartree-Fock), because Σ remains dynamical, i.e. frequency dependent, preserving local quantum fluctuations. The local approximation becomes exact in the limit of infinite spatial dimensionality and maps the interacting lattice model onto a self-consistent single impurity model like, for example, the Wolff model [24]:

$$\hat{H}_{\text{Wolff}} = \sum_{\vec{k}\sigma} \varepsilon_{\vec{k}} \hat{n}_{\vec{k}} + U(\hat{n}_{0\uparrow} - \frac{1}{2})(\hat{n}_{0\downarrow} - \frac{1}{2}) + \varepsilon(\hat{n}_{0\uparrow} + \hat{n}_{0\downarrow}). \tag{2.6}$$

Here, the one-particle energies $\varepsilon_{\vec{k}}$ have to be defined such that the non-interacting local Green function of the Wolff model fulfills $G^0_{\text{Wolff}} \equiv (G_{ii} - \tilde{\Sigma})^{-1}$. In the self-consistent solution the local (interacting) Green function of the Wolff model has to be equal to G_{ii}. In the presence of disorder one has to average over all possible values of U or ε, respectively. This type of local averaging is equivalent to the "coherent potential approximation", well known from investigations of disordered alloys.

While the self-consistency is rather easily reached by iteration the solution of the single impurity problem is the hard part. There exists no analytic solution and different numerical and approximative techniques have been employed [23]. Here we again use auxiliary field QMC [25], an algorithm quite similar to the one for finite dimensional lattices sketched above. The computer time grows like L^3 where the number of Matsubara frequencies, $L \propto \beta$. Fortunately, QMC for the single band model is free from the minus-sign problem.

In the following, the non-interacting DOS is chosen as a semi-elliptic model DOS with bandwidth=8, equal to the $d = 2$ tight binding bandwidth for $t = 1$. A typical quantity under consideration is the staggered magnetic susceptibility χ_{AF} whose divergence signals the transition to an AF ordered state. One can also extend the DMFT equations to the ordered phase to obtain spin and sublattice dependent electron densities and the sublattice magnetization M. The one-particle density of states (DOS) is obtained by analytical continuation of the imaginary time Green function using the Maximum Entropy method. For details of the algorithm, the implementation of disorder averages and determination of expectation values see [23,14].

3 Random Potentials

3.1 Local Moment Quenching

Random potentials are the most frequently studied type of disorder in the context of Anderson localization. Contrary to the Hubbard interaction which at half-filling favors single occupation on each site, different local potentials lead to different occupations and hence to a quenching of local magnetic moments on sites with large absolute value of the local potential. This is seen in Fig. 1a where the average local moment squared, m^2, is plotted versus disorder strength for a flat distribution of ε values with width Δ. It is also shown that the spin-spin-correlations go in parallel with m^2. For a large width of random potentials this type of disorder is apparently very effective in the destruction of magnetic order. To study the behavior of the charge gap, the electronic compressibility, $\kappa \equiv \partial n/\partial \mu$, is calculated as a function of Δ (Fig. 1b). While disorder decreases κ in the non-interacting case, κ is enhanced by disorder at finite U. The reason is the introduction of states within the AF charge gap as will be discussed below. As mentioned above, random potentials break the particle-hole symmetry leading to a minus-sign problem even at half filling. This is the reason why only small lattices (4×4 in Fig. 1) can be studied for this type of disorder.

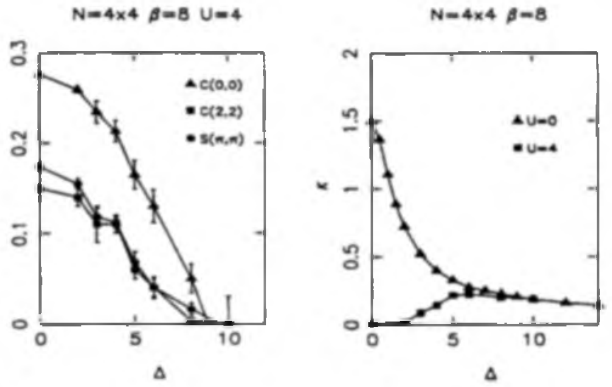

Figure 1 (a) Local magnetic moment $C(0,0)$, spin-spin correlation function at largest possible distance (2,2), and AF structure factor $S(\pi,\pi)$ as a function of disorder strength for a constant distribution of random potentials (in all cases the values at $U = \Delta = 0$ subtracted). (b) compressibility κ vs. Δ; disorder reduces κ in the non-interacting case and enhances it at $U = 4$ [16].

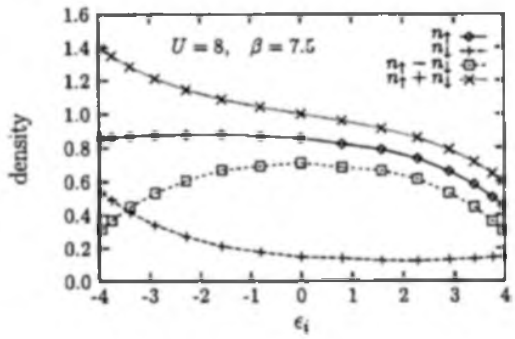

Figure 2
Local spin resolved densities in DMFT as a function of the random potential value ϵ_i [26]. Width of disorder distribution is $\Delta = 8$(=bandwidth).

3.2 Disorder-Enhanced Delocalization

Consider the situation deep in the AF phase, i.e. with a large staggered moment. A high value of the local potential on a given site reduces the potential barrier for a majority spin electron to tunnel to a neighboring sites. The electron is hence delocalized and the local magnetic moment is reduced. A low potential on the other hand cannot significantly further localize the majority spin because it is already almost saturated. This asymmetry of the localizing and delocalizing effects of random potentials is depicted in the DMFT results, Fig. 2. The majority spin ($\uparrow$) is strongly reduced for $\varepsilon > 0$ but almost unchanged for $\varepsilon < 0$. Note that the total local density monotonically decreases with ε, and that the net magnetization $(n_\uparrow - n_\downarrow)$ is reduced for any $|\varepsilon| > 0$.

The fact that the delocalization is not compensated can be expressed in terms of an enhanced effective hopping parameter t_{eff}. In the case $(U - \Delta) \gg t$ the effective t_{eff} can be estimated by the mapping onto the AF Heisenberg model: the AF exchange arises from virtual hopping of an electron with spin σ to a neighboring site occupied with an electron of spin $-\sigma$. The exchange energy for this and the opposite process is

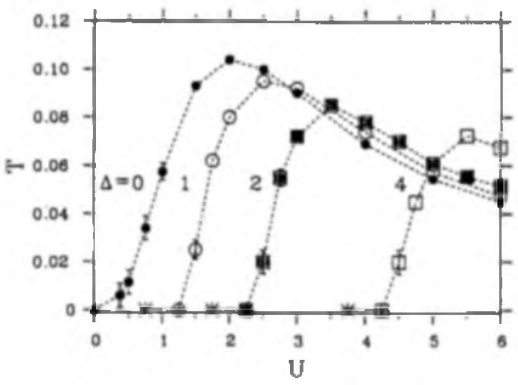

Figure 3
AF $(T-U)$ phase diagram in DMFT for a bimodal random potential distribution. Energies in units of the half bandwidth. [14]

$$J_{ij} = \frac{t^2}{U-(\varepsilon_i-\varepsilon_j)} + \frac{t^2}{U-(\varepsilon_j-\varepsilon_i)} \approx \frac{2t^2}{U}\left[1+\frac{(\varepsilon_i-\varepsilon_j)^2}{U^2}\right]. \tag{3.7}$$

J_{ij} is hence always *enhanced* from the pure case ($J_0 = 2t^2/U$), and the average exchange becomes $J_{av} = J_0[1+\lambda(\Delta/U)^2]$ where λ depends only on the shape of the disorder distribution (e.g., $\lambda = 1/12$ for the constant, $\lambda = 1/2$ for a binary distribution). Furthermore, one can show that the form of the magnon propagator remains unchanged in second order in Δ/U [26], but magnons are stiffened by a factor of $(1+\lambda(\Delta/U)^2)$. The effective hopping in strong coupling can thus be expressed as $t_{\text{eff}} = t[1+\lambda(\Delta/U)^2]^{1/2}$. In dimensions $d > 2$ one expects the Néel temperature T_N to be proportional to J and hence T_N, too, should be enhanced by weak disorder.

While disorder-enhanced delocalization stabilizes AF order at strong coupling it suppresses it at weak coupling. For small U the AF state is rather "spin density wave like" and an enhanced kinetic energy tends to weaken AF order and to reduce T_N. In addition, random potentials destroy the perfect nesting instability responsible for AF order at small U.

The T vs. U phase diagram within DMFT (Fig. 3) summarizes and confirms the above considerations: For small U, T_N is reduced and eventually vanishes when Δ becomes roughly equal to U. At large U, however, the T_N curves for different Δ cross each other, i.e. at a given value of U, T_N increases with disorder. The opposite effects of disorder on T_N depending on U are due to the non-monotonic behavior of the function $T_N(U)$. If the slope of $T_N(U)$ is positive (negative) an effectively reduced ratio U/t_{eff} leads to a suppression (enhancement) of T_N.

3.3 Closing of the Charge Gap

Local potentials can induce electronic states in the charge gap. As also found experimentally the positions of the impurity states are crucial for the stability of AF order with respect to carrier doping. Disorder-induced gap states will reduce the size of the charge gap. We now want to determine the critical disorder strength at which the gap vanishes. First we treat the disorder within the T-matrix approximation which becomes exact for a single impurity [27,26]. Since the local host Green function of the correlated, not-disordered

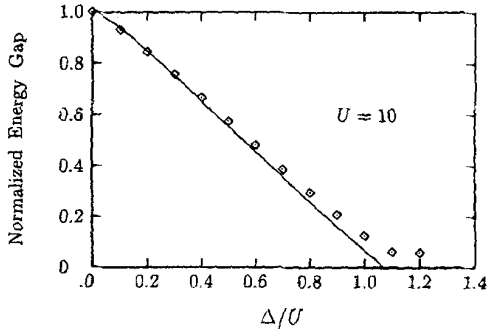

Figure 4
Normalized energy gap, $\tilde{D}/D$, in $d = 2$ versus disorder strength Δ at $U = 10t$ as obtained by the T-matrix approximation (solid line) and the UHF analysis (symbols) [26].

problem is unknown we approximate it by the Green function of the AF Hartree-Fock solution:

$$[g^0_\sigma]_{ii} = (1/N)\sum_{\vec{k}}(\omega - \sigma D)/(\omega^2 - E^2_{\vec{k}}). \tag{3.8}$$

Here $2D = mU$ is the Hubbard energy gap in the pure AF, $E_{\vec{k}} = \sqrt{D^2 + \varepsilon^2_{\vec{k}}}$ is the AF band energy, and D is obtained from the self-consistency condition $(1/N)\sum_{\vec{k}}(2E_{\vec{k}})^{-1} = U^{-1}$. With this local host Green function we can calculate the location of impurity-induced states from the poles in the T-matrix, $T_\sigma(\omega) = \varepsilon_i/(1 - \varepsilon_i[g^0_\sigma(\omega)]_{ii})$. We consider a constant distribution of random potentials between $\pm\Delta/2$. There are disorder-induced states within the gap if $|[g^0_\sigma]_{ii}| > 2/\Delta$. The energy $\tilde{D}$ up to which states are formed within the gap is given by $[g^0_\sigma(-\tilde{D})]_{ii} = 2/\Delta$. The remaining charge gap $2\tilde{D}$ is plotted versus Δ in Fig. 4. The decrease is almost linear and $2\tilde{D}$ vanishes close to $\Delta = U$. Also shown is the result from a numerical unrestricted Hartree-Fock (UHF) analysis. In this approach, the HF Hamiltonian on a finite lattice is numerically (self-consistently) diagonalized, so that disorder is treated exactly [10,11,26]. The energy gap is obtained from the energy difference between the lowest energy state of the upper Hubbard band and the highest energy state of the lower Hubbard band. Averages are taking over 100 disorder realizations on a 10×10 lattice. The saturation of the gap at $\Delta/U \sim 1$ is due to the finite system size. The agreement with the T-matrix approach is excellent for the present interaction value $U = 10t$. Deviations from the T-matrix approach are more pronounced at lower interaction strengths where the fermion states are more extended.

The closing of the charge gap is also observed within the DMFT approach. Fig. 5a shows the density of states for several disorder values. Note that all spectra shown are within the AF ordered phase, i.e. AF order is much more stable than the charge gap which closes about $\Delta = U$. A linear reduction of the charge gap is also observed in the case of a binary disorder distribution (Fig. 5b). For this stronger type of disorder both the charge gap and the AF order vanish near $\Delta = U$.

3.4 Spin Vacancies

As discussed in the previous section the one-particle excitation gap decreases with Δ and vanishes near $\Delta = U$. Upon further increase of Δ the two Hubbard bands will overlap whereby electrons from the highest levels of the lower band (with $\varepsilon_i > U/2$) will be

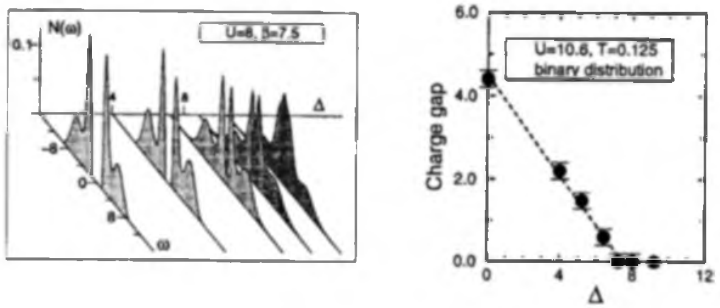

Figure 5 (a) Density of states (DOS) for a constant disorder distribution of different width in DMFT [26]; all spectra are within the AF phase. (b) Charge gap vs. Δ in DMFT for the bimodal distribution of random potentials.

transfered to the lowest levels of the upper band (with $\varepsilon_i < -U/2$). Those sites will become doubly occupied, their local moment will vanish as observed in Sec. 3.1. In the limit $t \ll U,\Delta$ the Hubbard bands at $\pm U/2$ are nearly flat with width Δ. The overlap region is $\sim (\Delta - U)$ and the fraction of nonmagnetic sites can be estimated by $x \sim (\Delta - U)/\Delta$.

In the following this situation is modeled by spin vacancies of concentration x which will lead to strong magnon scattering. Such diluted antiferromagnets have been widely studied recently mostly within spin diluted Heisenberg models [28,29] and also Hubbard models [27]. A perturbative analysis in the strong coupling limit ($O(t^2/U)$) [27,26] yields a softening of magnons by a factor of $(1 - 2x)$ in $d = 2$. Extrapolating to large fractions x, the magnon energy scale $\tilde{J} = J(1 - 2x)$ hence vanishes only close to the percolation threshold $x_{\text{perc}} \approx 0.4$. In $d > 2$ the Néel temperature is assumed to be proportional to $\tilde{J}$ and a linear decrease of T_N is thus expected. In experiments, e.g. on Li doped NiO [30] such a linear dependence on x is indeed observed with prefactor of 2.2. In the limit $d \to \infty$ the percolation threshold is 1.0; hence we can expect AF order to persist for arbitrarily large dilution. Within DMFT, too, a linear decrease of $T_N \propto (1 - x)$ is observed for the diluted model at large U (Fig. 6a). At small U, however, AF order is remarkably robust, T_N being constant up to dilutions close to $x = 1$ where T_N eventually drops to zero. This behavior

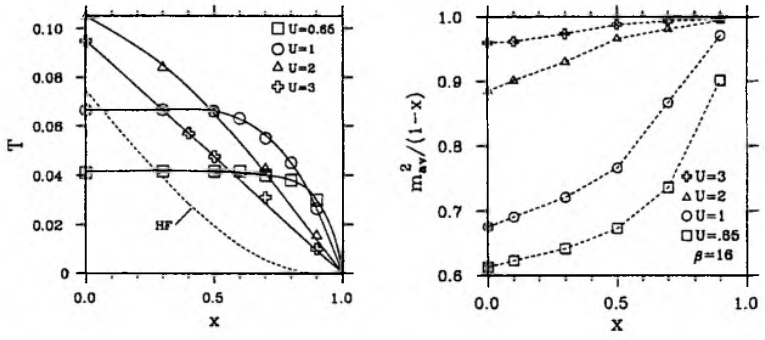

Figure 6 (a) T_N as a function of site dilution in DMFT for different values of U. Dashed line Hartree-Fock approximation for $U = 0.65$ (energies in units of the half bandwidth). (b) Enhancement of local moments on the remaining fraction $(1 - x)$ of the lattice at inverse temperature $\beta = 16$. [14]

of T_N can be explained by a strong enhancement of the local moment density on the remaining sites at small U (Fig. 6b). The reason for this enhancement is that with reduced average number of nearest neighbors the kinetic energy decreases, leading to a stronger localization. At large U the local moments are already almost saturated at $x = 0$ and just cannot be further enhanced. The situation in the case of vacancies is therefore quite different from the effect of weak site disorder where disorder-enhanced *delocalization* is observed.

4 Random Hopping

The case of spin vacancies discussed in the previous section can of course be regarded as a specific type of randomness in the hopping elements. The more generic case of a continuous (flat) distribution of $t_{ij} \in [1-\Delta/2, 1+\Delta/2]$ was studied in $d = 2$ using QMC. Since the hopping is still restricted between nearest neighbors on a square lattice particle-hole symmetry is preserved and no minus-sign problem occurs at $n = 1$. Random t_{ij} hardly affect the density of local moments (Fig. 7a), the slight decrease may be due to the enhanced kinetic energy which is $\propto \sqrt{\langle t_{ij}^2 \rangle}$. Nevertheless, longer-range spin-spin correlations are strongly suppressed if Δ is of the order of t (see Fig. 7a). The finite size scaling according to (2.4) yields the AF order parameter (staggered moment) M versus Δ (Fig. 7b). M vanishes at a critical disorder strength of $\Delta_c \approx 1.4$. We propose [16] that the phase boundary is determined basically by the variance of the AF exchange coupling $\nu = (\langle J_{ij}^2 \rangle - \langle J_{ij} \rangle^2)/\langle J_{ij}^2 \rangle$. AF order persists for $\nu < \nu_c \approx 0.4$. This criterion is consistent with the phase boundary of the bond-disordered AF Heisenberg model with a bimodal distribution of J_{ij} [31]. The reason for the vanishing of AF order for this type of disorder is supposedly the formation of local singlets. Such singlets will form first on the strongest bonds and will leave some spins which are weakly coupled to their neighbors unpaired. Those "free" spins are expected to give a Curie-like contribution to the susceptibility as observed in doped semiconductors [18,19]. The numerical results indeed show a strong enhancement of the uniform susceptibility in the disordered case [16].

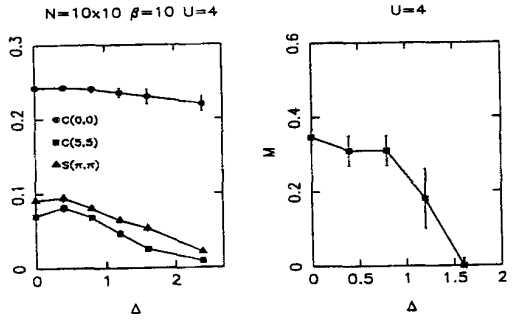

Figure 7 (a) Local moment and spin-spin correlations in $d = 2$ for random hopping (same quantities as in Fig. 1). (b) Staggered magnetization M vs. Δ as obtained by finite size scaling [16].

5 Impurities with Weak Local Interactions

The Hubbard model at $n = 1$ exhibits both AF order and the Mott-Hubbard metal-insulator transition (MIT). It is important to note that both effects are in principle independent. The Mott-Hubbard MIT occurs at intermediate interaction ($U \sim$ bandwidth) while AF order can set in at arbitrarily small U due to the Fermi surface nesting instability. It is argued that the MIT at $T = 0$ represents a quantum critical point which is however concealed by the low temperature AF phase [32], and attempts are made to suppress the AF phase to very low or zero T by different types of frustration [23]. A different possibility to separate AF order and the MIT is to shift the filling at which the Mott-Hubbard MIT occurs away from $n = 1$ by introducing impurities with a low (or zero) local interaction with a concentration f. Such impurity sites can be doubly occupied without the cost of the local repulsion and hence the MIT is expected at a density $n = 1 + f$.

5.1 Mott-Hubbard Gap

The Hubbard model with a bimodal distribution of U values ($U = 0$ on a fraction f of the lattice, and $U = 8t$ on the remaining sites) was investigated by QMC on square lattices and in DMFT. Note that for technical reasons (minus-sign problem) the choice of the U−disorder in model (1.1) preserves particle-hole symmetry. This corresponds to different chemical potentials on the two constituents such that at $n = 1$ the electronic density is homogeneous, i.e. independent of U_i. To detect charge gaps the electron density n is plotted versus the chemical potential μ (Fig. 8a). As expected the gap moves to a density off half filling close to $1 + f$. This agrees with the kinetic energy which shows minima at the corresponding densities (Fig. 8b). At a closer look one observes an additional gap at $n = 1$ which is due to the doubling of the unit cell in the AF ordered state. The gaps at $n = 1$ and $n = 1 + f$ can also be detected by the one-particle spectrum, obtained in DMFT [17]. Between densities 1 and $1 + f$ the systems is apparently compressible.

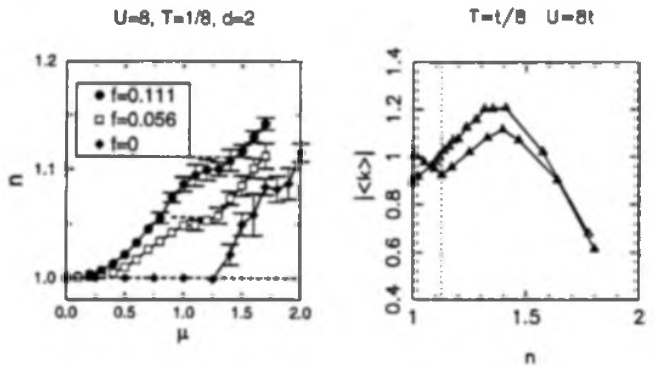

Figure 8 (a) Electron density n vs. chemical potential μ for different values of $U = 0$ impurity concentration f. $n(\mu)$ has plateaux at $n = 1$ and close to $n = 1 + f$. (b) Kinetic energy $\langle k \rangle$ vs. average density for $f = 0$ (open triangles) and $f = 0.111$ (solid triangles). $\langle k \rangle$ shows minima at $n = 1 + f$ [17].

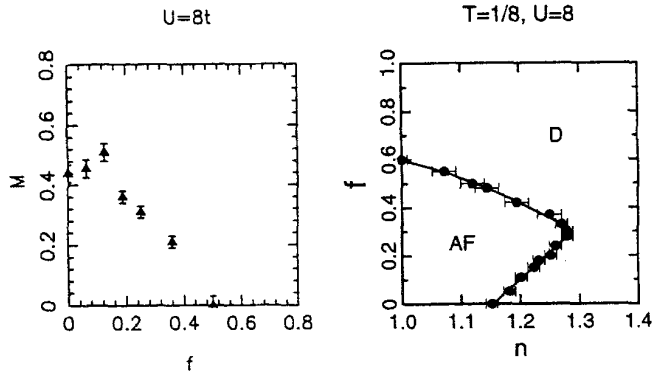

Figure 9 (a) Staggered magnetization in $d = 2$ as a function of impurity concentration f. (b) $f - n$ phase diagram at temperature $T = 1/8$ within DMFT. For small f the AF phase is stabilized against doping. [17]

5.2 Antiferromagnetic Order

Figure 9a shows the staggered moment M extrapolated to the thermodynamic limit in $d = 2$ at $n = 1$ as a function of impurity concentration f. For small f AF order is robust leading to the charge gap at $n = 1$. AF order vanishes at $f_c \approx 0.45$, i.e. close to the percolation threshold $f_{\text{perc}} \approx 0.4$.

Off half-filling the finite size scaling is no longer possible due to the minus-sign problem and the AF phase boundary is obtained within DMFT only (shown in Fig. 9b at $T = 1/8$). It is found that the $U = 0$ impurities can induce AF order at densities for which the clean model is disordered. In the clean model ($f = 0$) additional electrons are free to move and hence very effective in destroying long range order. $U = 0$ sites provide localizing centers which are energetically favorable for the additional carriers. This is why the AF phase extends to larger dopings at finite (but small) values of f. Since the mechanism of localizing mobile dopants is observed in $d = 2$, too, we expect the enlargement of the AF phase to be present in $d = 2$ at $T = 0$ as well, in spite of the fact that in the clean model in $d = 2$ the critical doping is supposed to be zero. Eventually at larger fractions f the AF phase shrinks, and the critical density approaches 1.0 for $f_c \approx 0.6$ ($f_c \approx 0.75$ in the ground state [17]). For even larger values of f there is no AF order even at $n = 1$.

Both the stabilization of AF order and the shift of the Mott gap to higher densities result from the localization of carriers at the $U = 0$ impurities. AF order is only destroyed when the density on the $U = 0$ sites saturates, i.e. it is stable *across* the Mott-Hubbard MIT. Hence the separation of Mott-Hubbard MIT and AF order is not present in the $U = 0$ impurity model, at least not for the present parameter values.

6 Summary and Conclusion

In this paper we discussed different types of disorder in correlated antiferromagnets and presented results obtained mostly by quantum Monte Carlo simulations in $d = 2$ and within dynamical mean-field theory ($d = \infty$).

Different mechanisms were identified by which disorder can enhance antiferromagnetic order: (i) disorder-enhanced delocalization at strong coupling in the case of weak disorder in the chemical potentials and (ii) localization of surplus carriers in the case of impurities with weak local interaction. In both cases compressible antiferromagnetic phases are observed. To determine if the gapless AF phase is metallic requires the calculation of transport properties which is presently in progress.

Quantum Monte Carlo simulations of electronic tight binding models are just making the transition from addressing rather abstract issues of correlation effects to making contact with real experiments. One important feature in this respect is the treatment of intrinsic disorder. For a quantitative description of experiments, however, the inclusion of a realistic band structure is mandatory. Here the DMFT will be particularly helpful because it allows for the treatment of multi-band models in a wider range of parameters and in the thermodynamic limit.

Bibliography

[1] G. Xiao, M. Z. Cieplak, A. Gavrin, F. H. Streitz, A. Bakhshai, and C. L. Chien Phys. Rev. Lett. **60**, 1446 (1988); B. Keimer et al., Phys. Rev. B **45**, 7430 (1992); A. V. Mahajan, H. Alloul, G. Collin, and J. F. Marucco, Phys. Rev. Lett. **72**, 3100 (1994).

[2] M. C. Martin, M. Hase, K. Hirota, G. Shirane, Y. Sasago, N. Koide, and K. Uchinokur, Phys. Rev. B **56**, 3173 (1997). P. E. Anderson, J. Z. Liu, and R. N. Shelton, Phys. Rev. B **56**, 11014 (1997).

[3] M. Azuma, Y. Fujishiro, M. Takano, M. Nohara, and H. Takagi, Phys. Rev. B **55**, 8658 (1997).

[4] H. Takagi et al., Phys. Rev. B **40**, 2254 (1989). S. Uchida et al., Phys. Rev. B **43**, 7942 (1991).

[5] T. Ido, K. Magoshi, H. Eisaki, and S. Uchida, Phys. Rev. B **44**, 12094 (1991).

[6] S. Hüfner, P. Steiner, I. Sander, F. Reinert, and H. Schmitt, Z. Phys. B **86**, 207 (1992); ibid. **88**, 247 (1992) F. Reinert et al., Z. Phys. B **97**, 83 (1995).

[7] M. Ma and E. Fradkin, Phys. Rev. B **28**, 2990 (1983); A. M. Finkelshtein, Zh. Eksp. Teor. Fiz. **84**, 168 (1983) [Sov. Phys. JETP **57**, 97 (1983)]; C. Castellani, C. Di Castro, P. A. Lee, and M. Ma, Phys. Rev. B **30**, 527 (1984); C. Castellani, C. Di Castro, and M. Grilli, *ibid.* **34**, 5907 (1986).

[8] A. M. Finkelshtein, Z. Phys. B **56**, 189 (1984); C. Castellani, et al. Phys. Rev. B **30**, 1956 (1984); **33**, 6169 (1986).

[9] M. Ma, Phys. Rev. B **26**, 5097 (1982); J. Yi, L. Zhang, and G. S. Canright, Phys. Rev. B **49**, 15 920 (1994).

[10] M. E. Tusch and D. E. Logan, Phys. Rev. B, **48**, 14 843 (1993).

[11] A. Singh and Z. Tešanović, Phys. Rev. B **41**, 614 (1990); **41**, 11 457 (1990), S. Basu and A. Singh, Phys. Rev. B **53**, 6406 (1996).

[12] V. Janiš and D. Vollhardt, Phys. Rev. B **46**, 15 712 (1992).

[13] V. Dobrosavljević and G. Kotliar, Phys. Rev. Lett. **71**, 3218 (1993); Phys. Rev. B **50**, 1430 (1994).

[14] V. Janiš, M. Ulmke, and D. Vollhardt, Europhys. Lett. **24**, 287 (1993); M. Ulmke, V. Janiš, and D. Vollhardt, Phys. Rev. B **51**, 10 411 (1995).

[15] A. Sandvik and D. J. Scalapino, Phys. Rev. **47**, 10090 (1993); A. Sandvik, D. J. Scalapino, and P. Henelius, Phys. Rev. **50**, 10474 (1994).

[16] M. Ulmke and R. T. Scalettar, Phys. Rev. B **55**, 4149 (1997).

[17] P. J. H. Denteneer, M. Ulmke, R. T. Scalettar, G. T. Zimanyi, Physica A **251**, 162 (1998); M. Ulmke, P. J. H. Denteneer, R. T. Scalettar, G. T. Zimanyi, Europhys. Lett. **42**, 655 (1998).

[18] D. Belitz and T. R. Kirkpatrick, Rev. Mod. Phys. **66**, 261, (1994).

[19] R. N. Bhatt and P. A. Lee, Phys. Rev. Lett. **48**, 344 (1982). M. Milovanović, S. Sachdev, and R. N. Bhatt, Phys. Rev. Lett. **63**, 82 (1989).

[20] R. Blankenbecler, D. J. Scalapino, and R. L. Sugar, Phys. Rev. **D 24**, 2278 (1981). J. E. Hirsch, Phys. Rev. **B 28**, 4059 (1983). G. Sugiyama and S.E. Koonin, Ann. Phys. **168**, 1 (1986); S. Sorella, S. Baroni, R. Car, and M. Parrinello, Europhys. Lett. **8**, 663 (1989). S. R. White, D. J. Scalapino, R. L. Sugar, E. Y. Loh, J. E. Gubernatis, and R. T. Scalettar, Phys. Rev. **B 40**, 506 (1989).

[21] D. A. Huse, Phys. Rev **B 37**, 2380 (1988).

[22] W. Metzner and D. Vollhardt, Phys. Rev. Lett. **62**, 324 (1989); D. Vollhardt, in *Correlated Electron Systems*, ed. V. J. Emery, World Scientific, Singapore, 1993.

[23] T. Pruschke, M. Jarrell, J. K. Freericks, Adv. Phys. **44**, 187 (1995); A. Georges, G. Kotliar, W. Krauth, M. Rozenberg, Rev. Mod. Phys. **68**, 13 (1996).

[24] P. A. Wolff, Phys. Rev. **124**, 1030 (1961).

[25] J. E. Hirsch and R. M. Fye, Phys. Rev. Lett. **56**, 2521 (1986).

[26] A. Singh, M. Ulmke, and D. Vollhardt, Phys. Rev. B **58** (to appear Oct. 1998); cond-mat/9803094.

[27] P. Sen, S. Basu, and A. Singh, Phys. Rev. B **50**, 10 381 (1994); P. Sen and A. Singh, Phys. Rev. B **53**, 328 (1996); A. Singh and P. Sen, Phys. Rev. B **57**, 10598 (1998).

[28] N. Bulut, D. Hone, D. J. Scalapino, and E. Y. Loh, Phys. Rev. Lett. **62**, 2192 (1989); D. Poilblanc, D. J. Scalapino, and W. Hanke, Phys. Rev. Lett. **72**, 884 (1994); G. B. Martins, M. Laukamp, J. Riera, and E. Dagotto, Phys. Rev. Lett. **78**, 3563 (1997). Y. Motome, N. Katoh, N. Furukawa, and M. Imada, J. Phys. Soc. Jpn. **65**, 1949 (1996).

[29] W. Brenig and A. P. Kampf, Phys. Rev. B **43**, 12 914 (1991); E. Manousakis, Phys. Rev. B **45**, 7570 (1992); C. C. Wan, A. B. Harris and D. Kumar, Phys. Rev. B **48**, 1036 (1993).

[30] M. Corti et al., Phys. Rev. B **56**, 11056 (1997).

[31] A. Sandvik and M. Vekić, Phys. Rev. Lett. **74** 1226 (1995).

[32] For a recent review see: F. Gebhard, *The Mott Metal–Insulator Transition*, Springer Tracts in Modern Physics, vol. 137 (Springer, Heidelberg, 1997).